Supplementary Figure 4. Plots of the increase in fractional saturation and comparison of the residuals to single and double exponential fits.

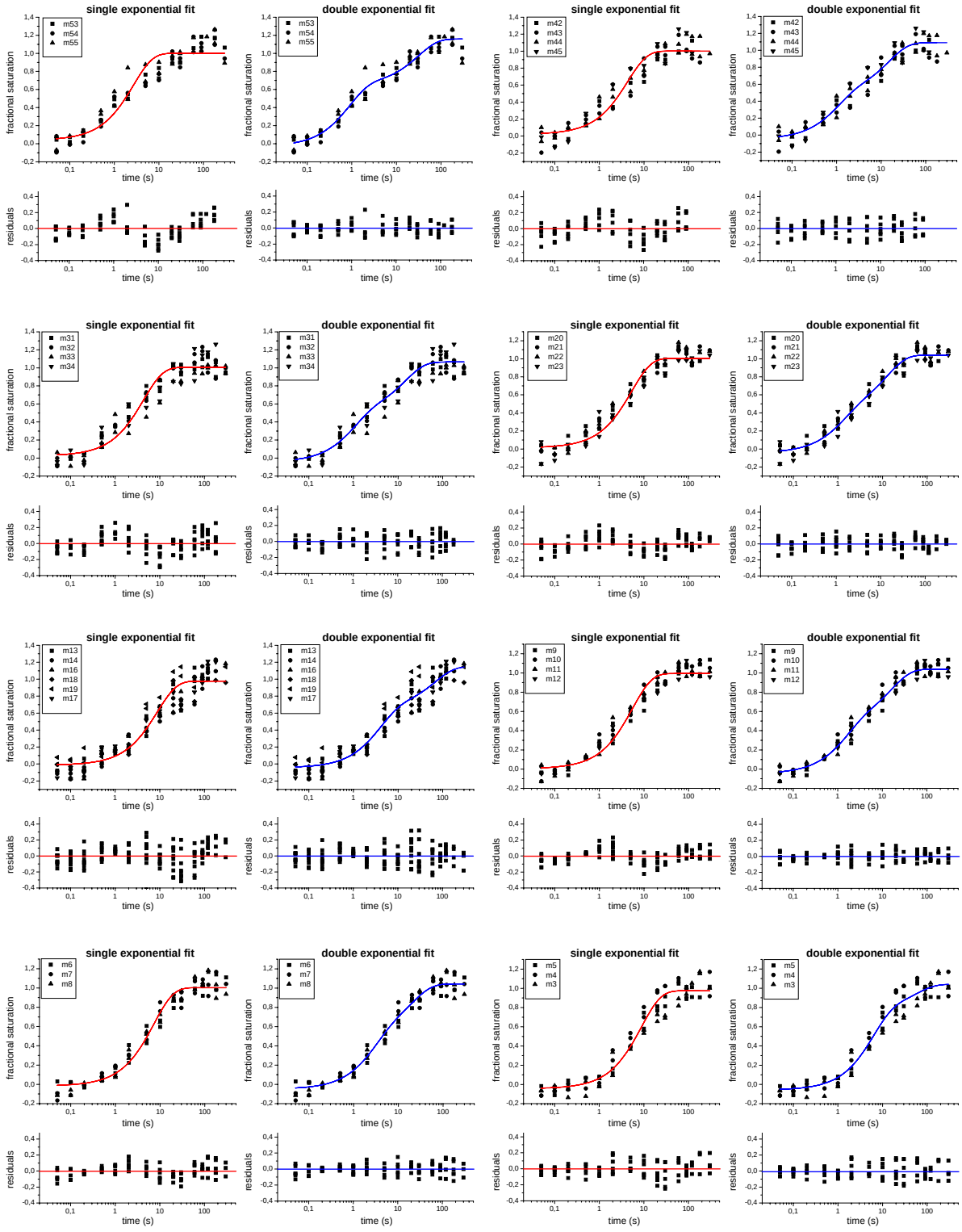

Figure 4A. Comparison of the fits of the kinetics of the appearance of protection at specific sites on the template strand upon *E.coli* RNAP binding to the wild type *A1* promoter of phage *T7* at 37°C to a single (red curve) and double (blue curve) exponential equation. Shown are the residuals (the difference between the data points and the fit curve, for details see "Data analysis") for the two fits.

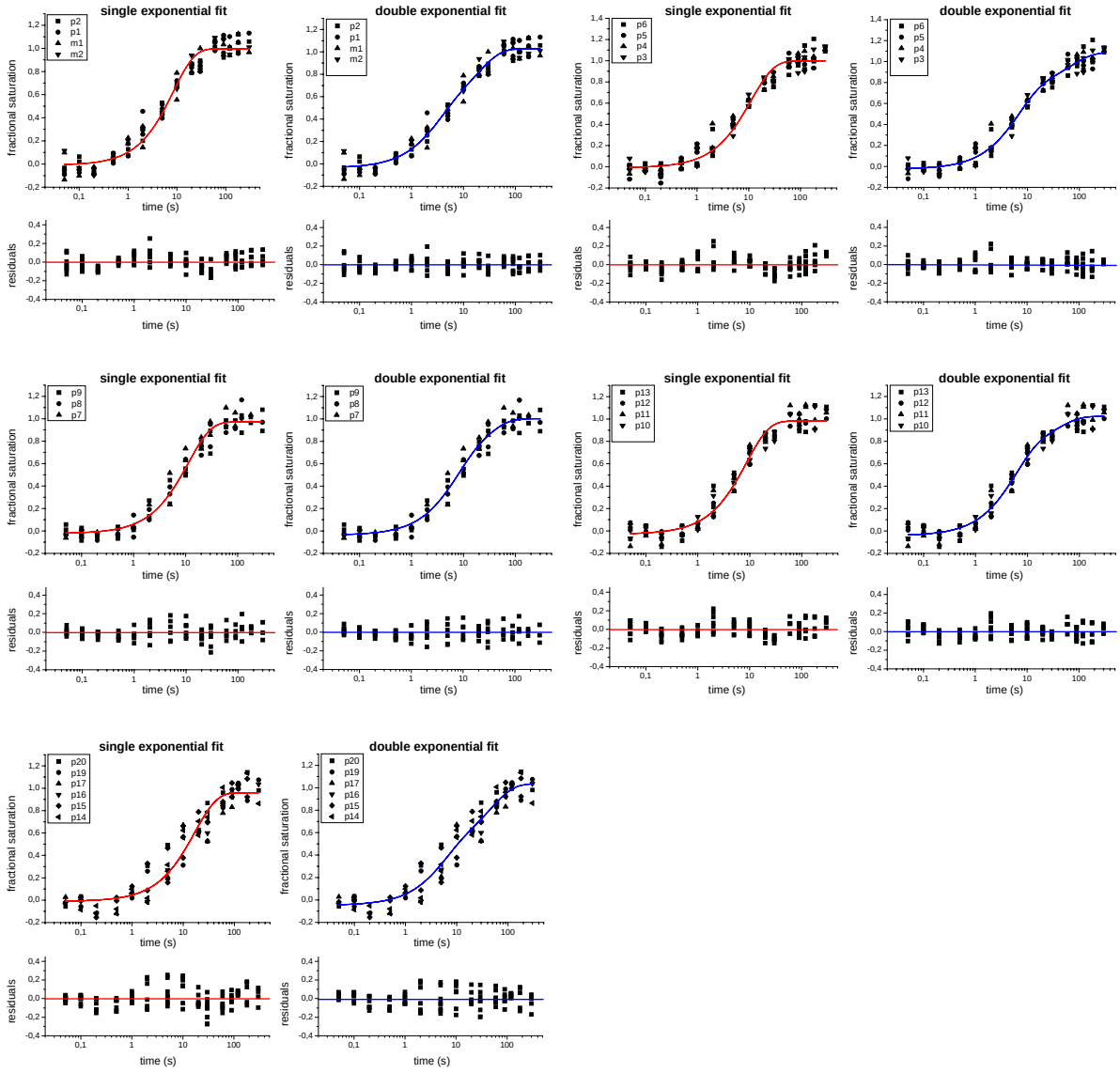

Figure 4A. (continuation).

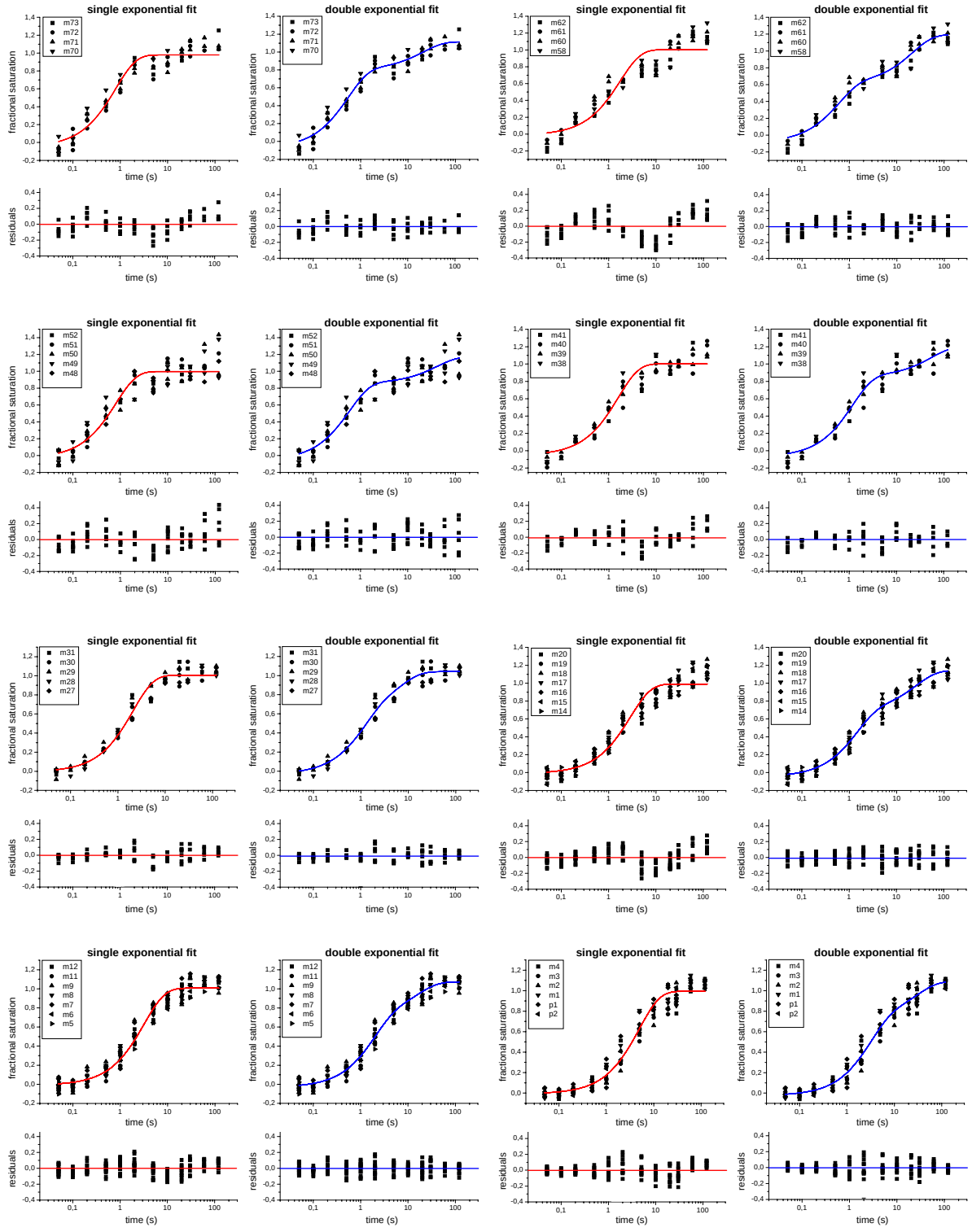

Figure 4B. Comparison of the fits of the kinetics of the appearance of protection at specific sites on the non–template strand upon *E.coli* RNAP binding to the wild type *A1* promoter of phage *T7* at 37°C to a single (red curve) and double (blue curve) exponential equation. Shown are the residuals for the two fits.

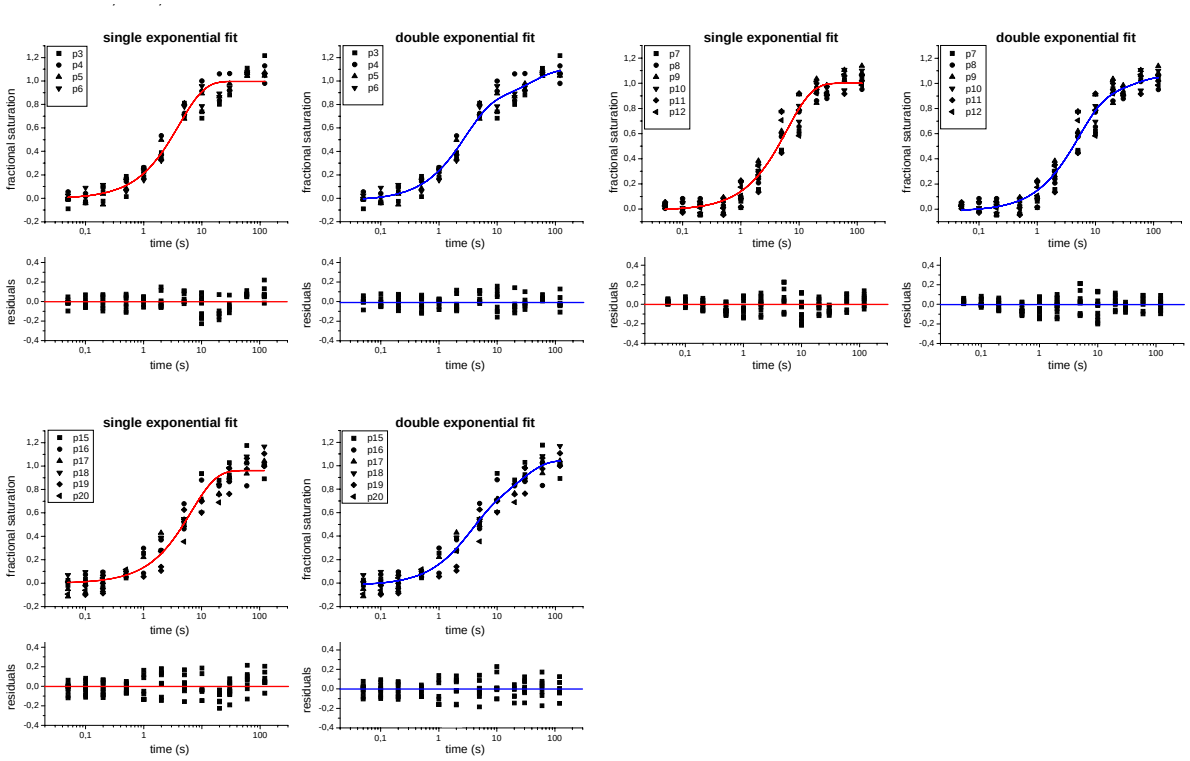

Figure4B (continuation).

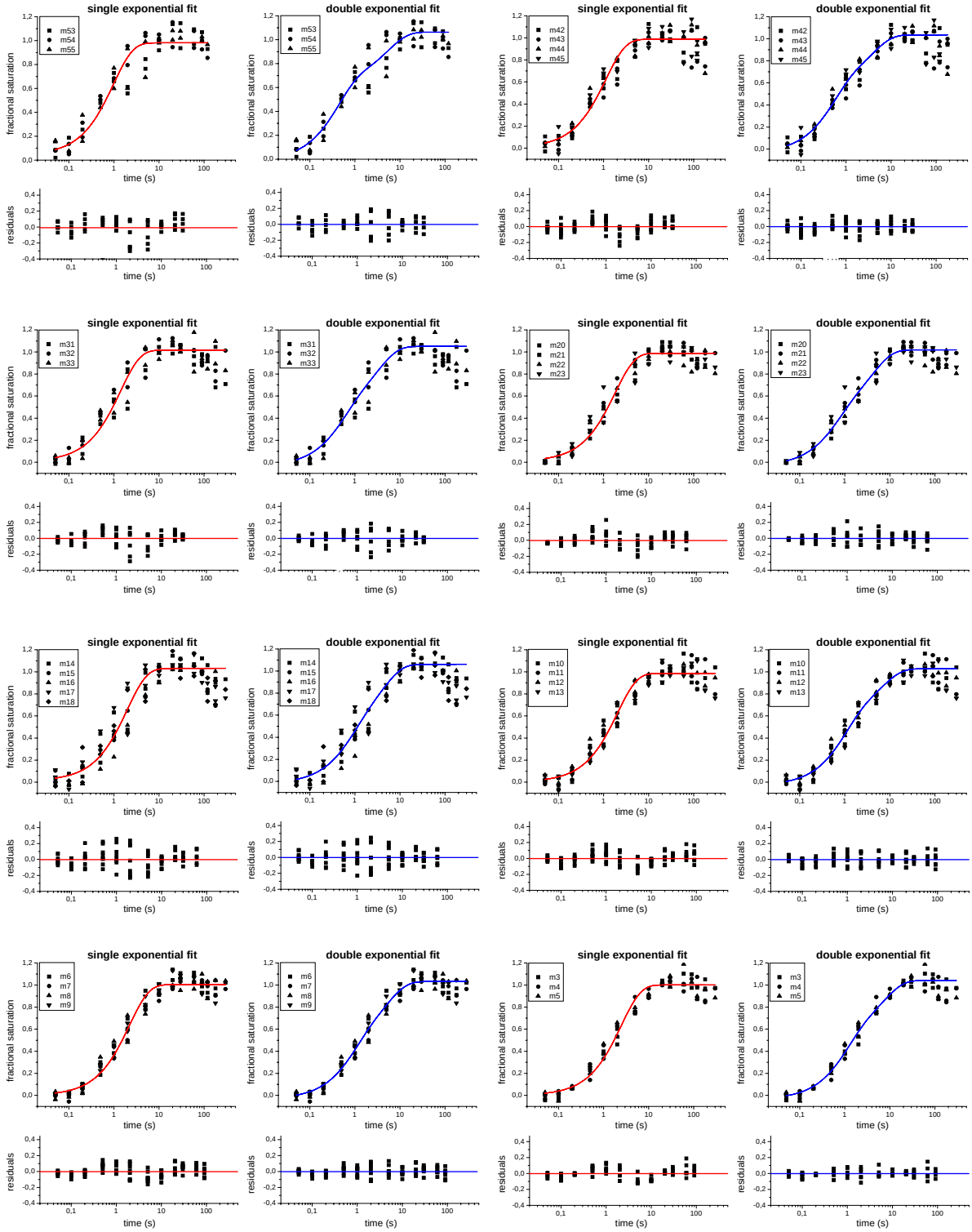

Figure 4C. Comparison of the fits of the kinetics of the protection appearance at specific sites on the template strand upon *E.coli* RNAP binding to the mutant–1 *T7A1* promoter at 37°C to a single (red curve) and double (blue curve) exponential equation. Shown are the residuals for the two fits (for details see section "Data analysis"). In the case that a decrease in fractional saturation was observed at the longer time points, the fits were carried out in the absence of the points in the decreasing portion of the curve.

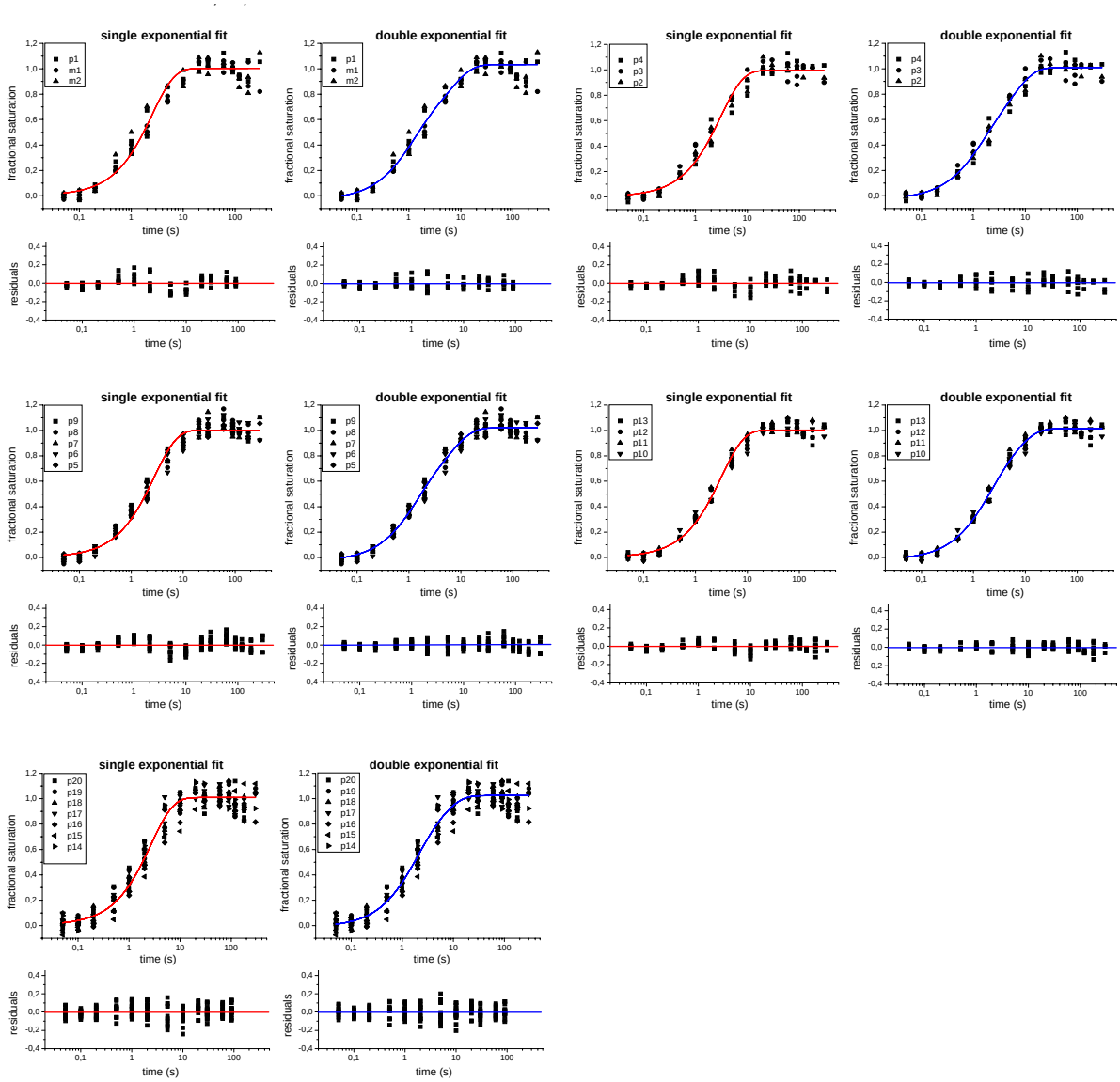

Figure 4C (continuation).

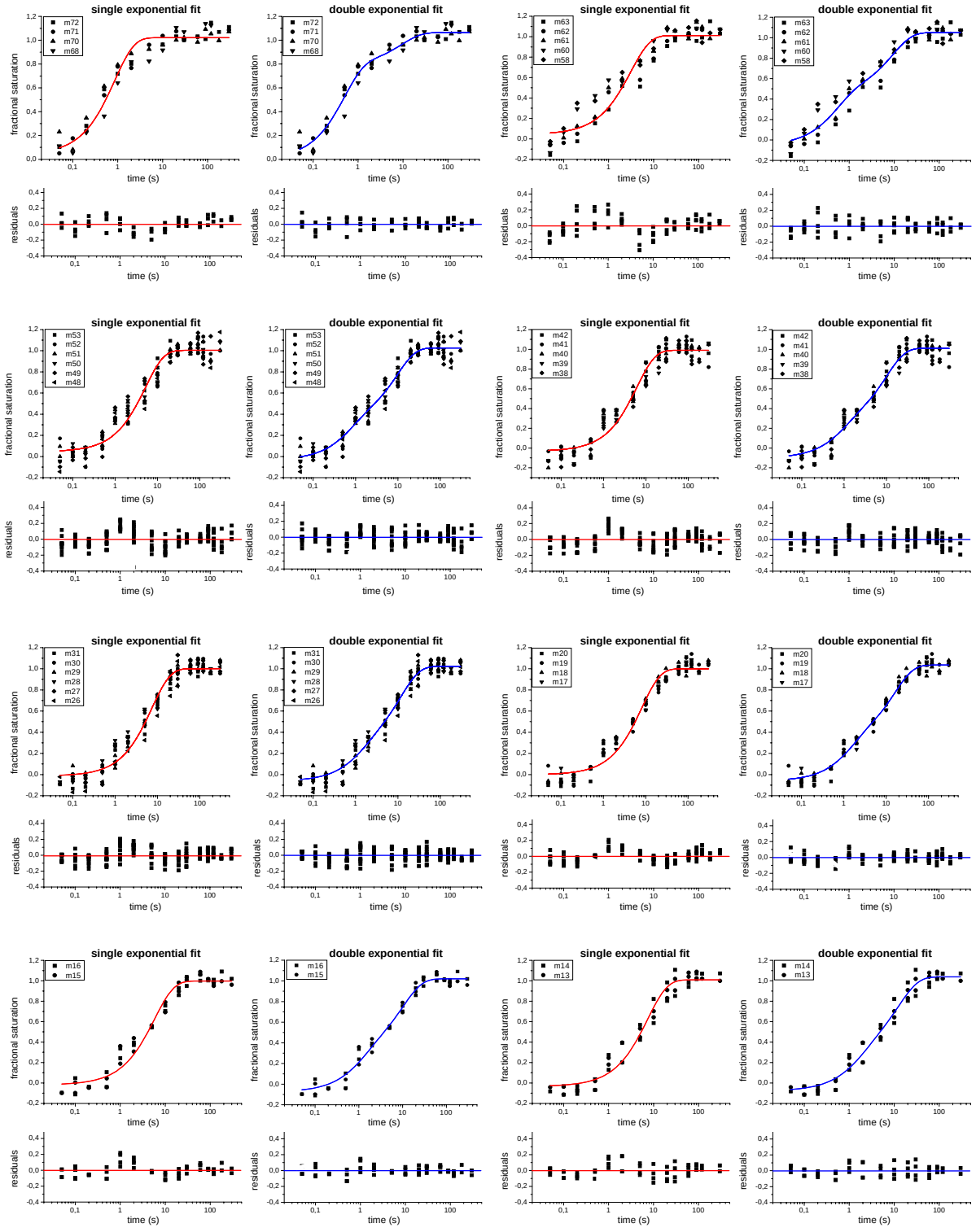

Figure 4D. Comparison of the fits of the kinetics of the protection appearance at specific sites on the non–template strand upon *E.coli* RNAP binding to the mutant–1 *T7A1* promoter at 37°C to a single (red curve) and double (blue curve) exponential equation. Shown are the residuals for the two fits (for details see section "Data analysis").

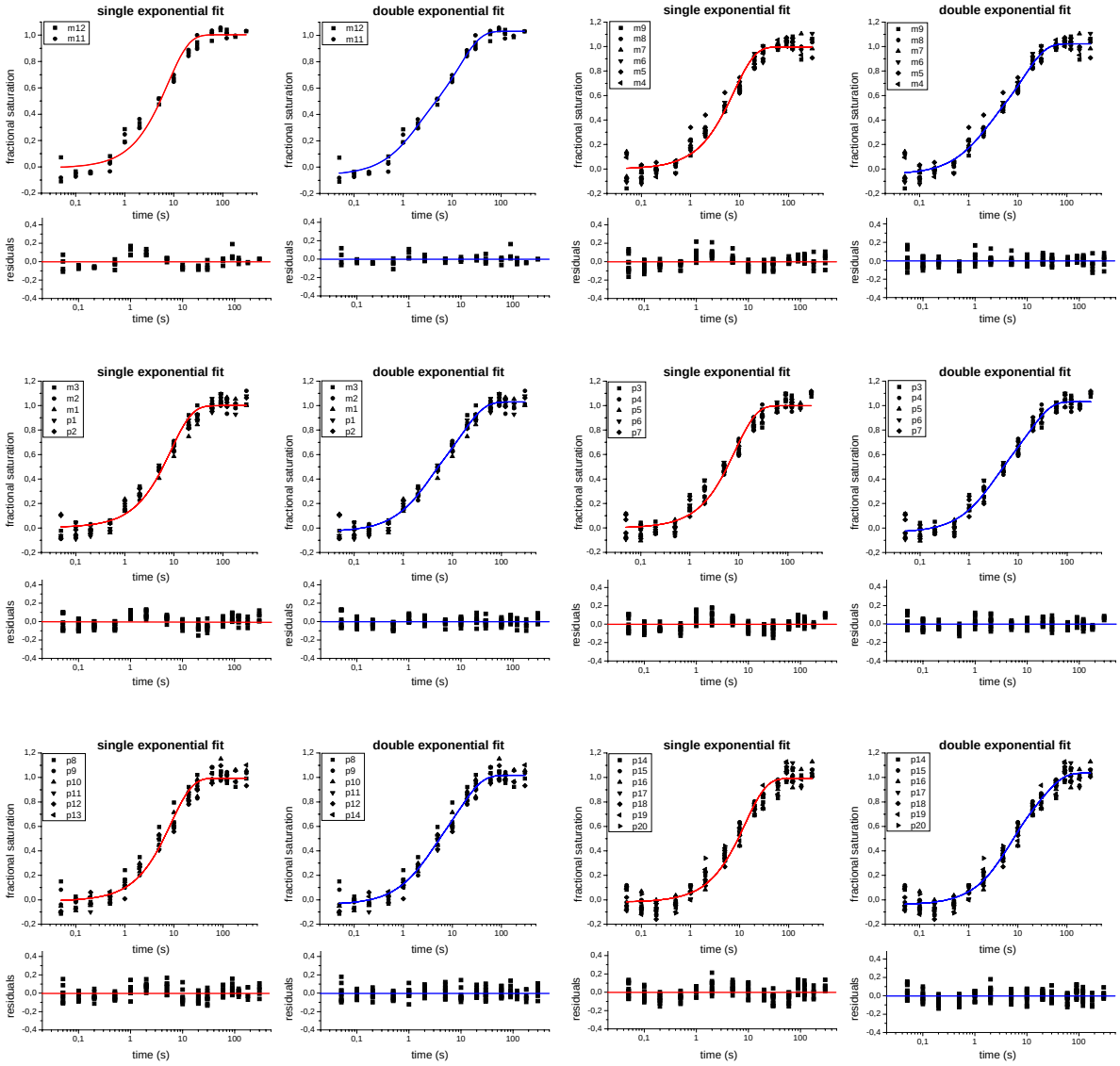

Figure 4D. (continuation).

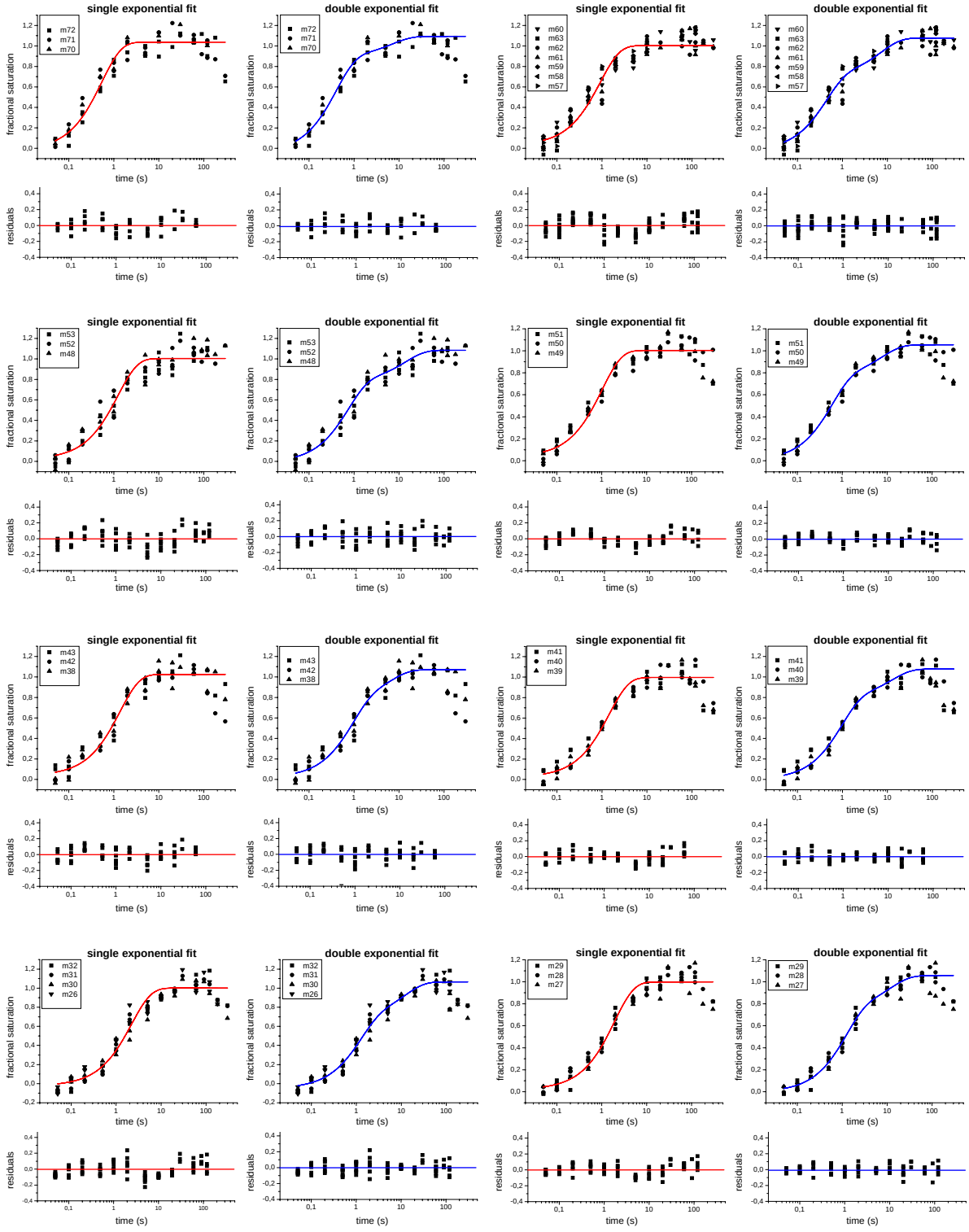

Figure 4E. Comparison of the fits of the kinetics of the appearance of protection at specific sites on the non–template strand upon *E.coli* RNAP binding to the wild type *T7A1* promoter at 20°C to a single (red curve) and double (blue curve) exponential equation. Shown are the residuals for the two fits (for details see section "Data analysis"). In the case then a decrease in fractional saturation was observed at the longer time points, the fits were carried out in the absence of the points in the decreasing portion of the curve.

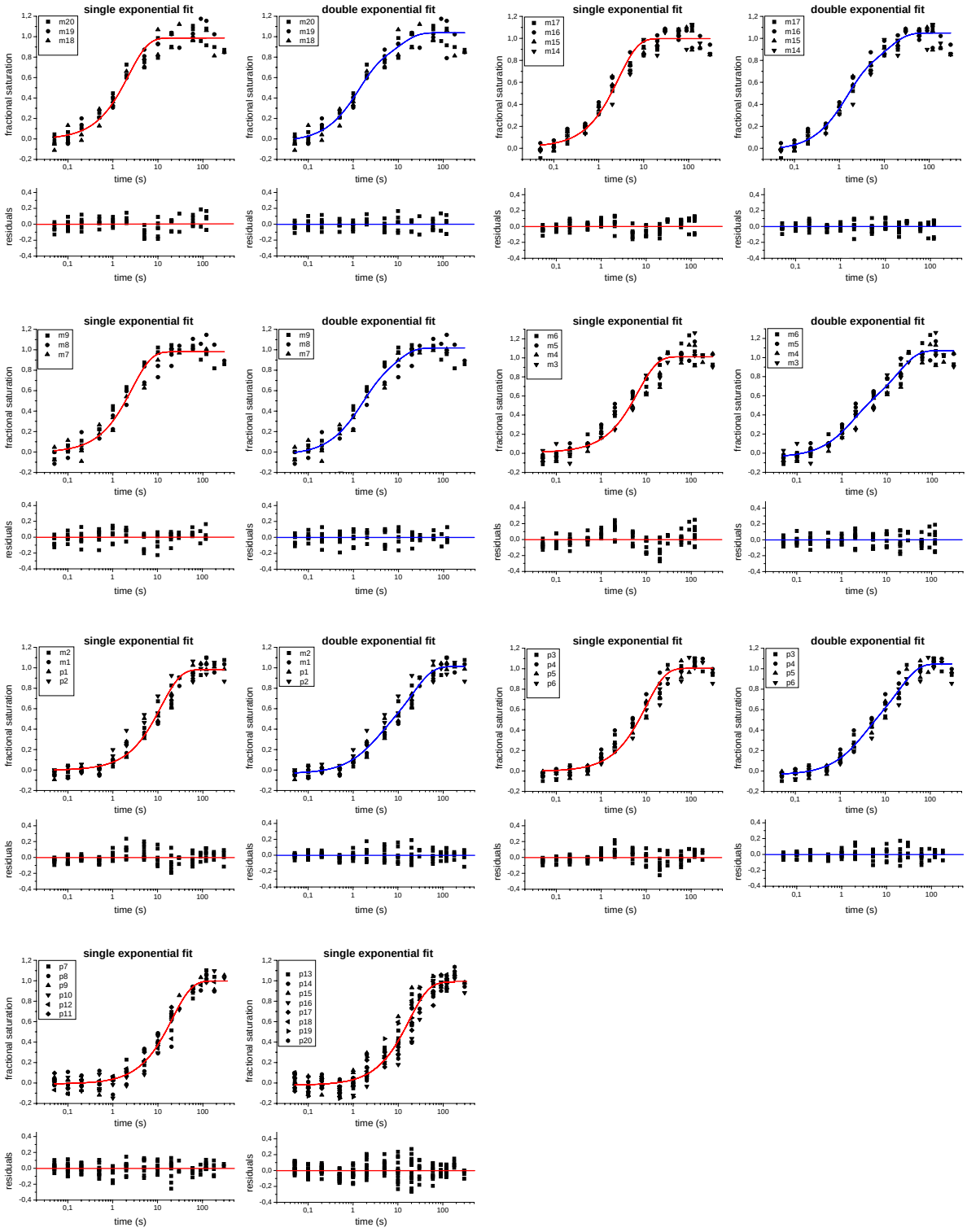

Figure 4E. (continuation).

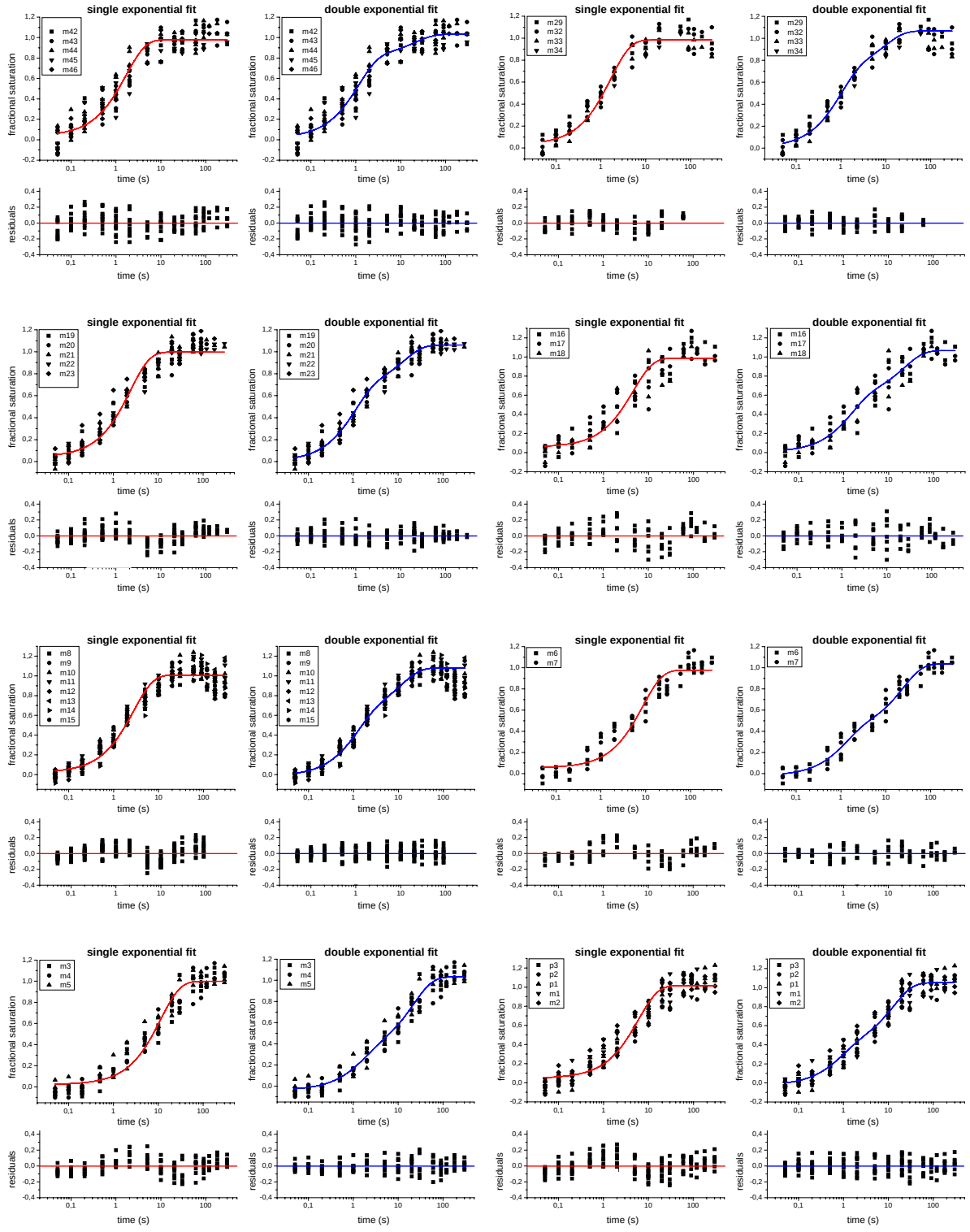

Figure 4F. Comparison of the fits of the kinetics of the appearance of protection at specific sites on the template strand upon *E.coli* RNAP binding to the wild type *T7A1* promoter at 20°C to a single (red curve) and double (blue curve) exponential equation. Shown are the residuals for the two fits. In the case then a decrease in fractional saturation was observed at the longer time points, the fits were carried out in the absence of the points in the decreasing portion of the curve.

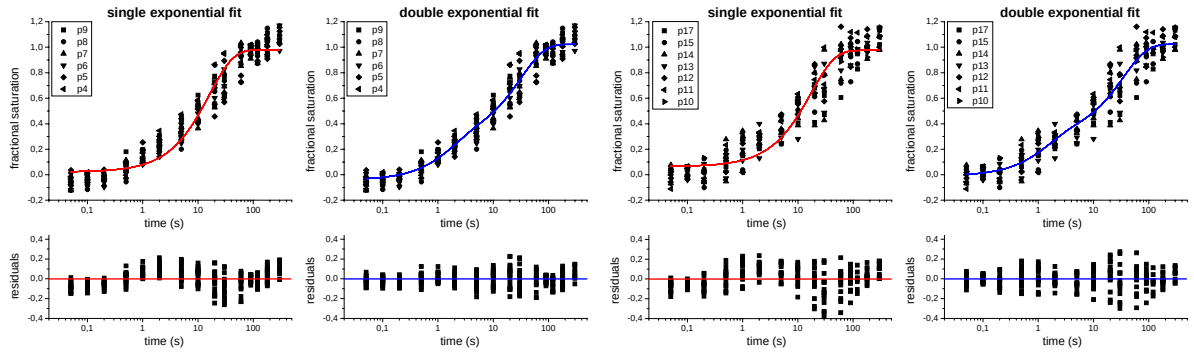

Figure 4F. (continuation).

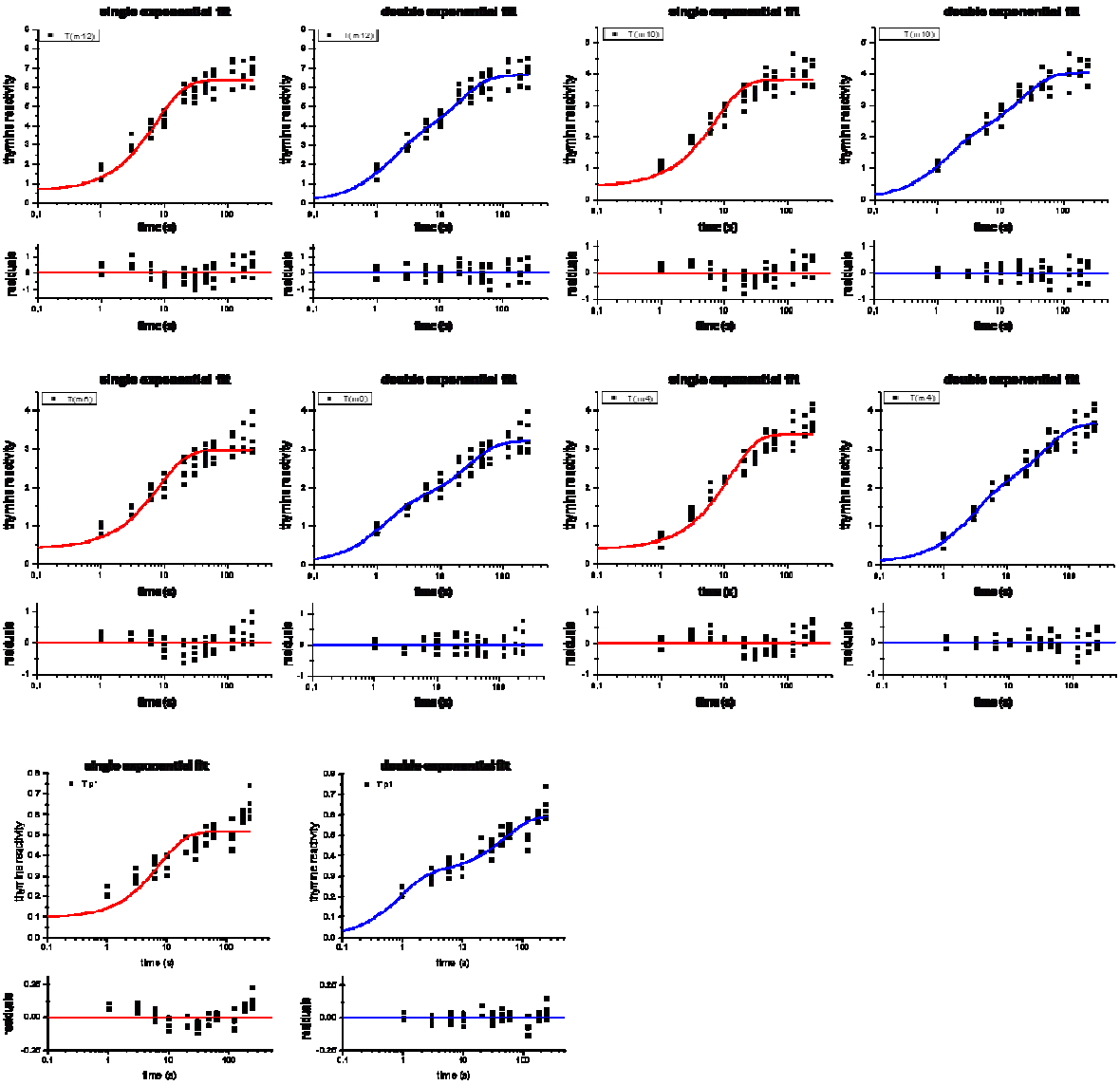

Figure 4G. Comparison of the fits of the kinetics of increase of template strand thymines reactivity to $KMnO_4$ upon open complex formation on the wild type *T7A1* promoter at 37°C to a single (red curve) and double (blue curve) exponential equation. Shown are the residuals for the two fits (for details see section "Data analysis").

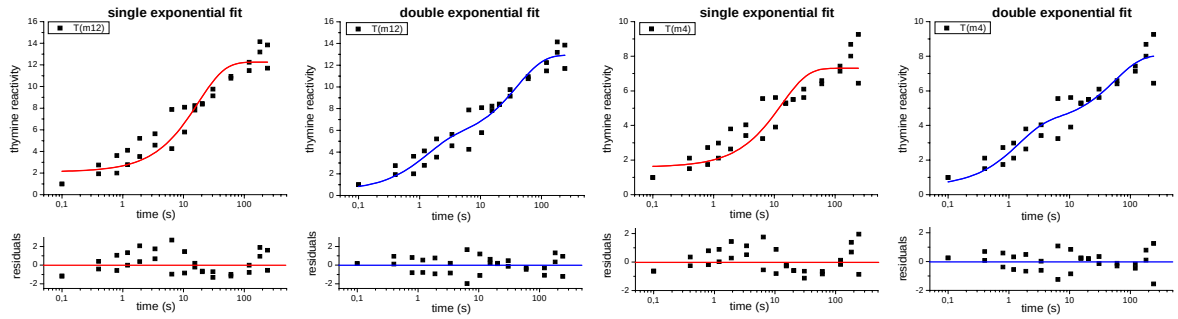

Figure 4H. Comparison of the fits of the kinetics of increase of template strand thymines reactivity to $KMnO_4$ upon open complex formation on the *T7A1* promoter with the consensus -10 region at 37°C to a single (red curve) and double (blue curve) exponential equation. Shown are the residuals for the two fits (for details see section "Data analysis").